JMEPEG (2006) 15:9-12
DOI: 10.1361/105994906X83484

1059-9495/$19.00

# An Adaptive Constitutive Model of the Ti-6.29Al-2.71Mo-1.42Cr Alloy in High-Temperature Deformation

*M.Q. Li, Aiming Xiong, and Xiaoli Li*

*(Submitted July 26, 2005; in revised form September 9, 2005)*

**In this paper, an adaptive constitutive model has been acquired with the help of a fuzzy set and an artificial neural network, so as to represent the deformation behavior of the Ti-6.29Al-2.71Mo-1.42Cr alloy in high-temperature deformation. In establishing this model for the constitutive relationship of this alloy, the process parameters of deformation temperature, strain rate, and strain were taken as three inputs, and the flow stress was taken as an output. Data from "teaching samples" and testing samples were obtained from the experimental results in the isothermal compression of the Ti-6.29Al-2.71Mo-1.42Cr alloy. By comparison of the calculated results with the experimental data from the testing samples, it was verified that the present adaptive constitutive model to predict the flow stress of the Ti-6.29Al-2.71Mo-1.42Cr alloy has good learning precision and generalization.**

**Keywords** flow stress, high-temperature deformation, model, titanium alloy

## 1. Introduction

The constitutive relationships describing the flow stress behavior of materials during hot deformation are usually nonlinear and complex, owing to dynamic variation in the microstructure during plastic deformation, particularly in superalloys. Picu proposed a physically based model for the plastic deformation of Ti6Al4V alloy (Ref 1). Ellyin and Xia presented a rate-dependent elastic-plastic constitutive model to be implemented into a finite-element code (Ref 2). Zhou formulated constitutive modeling of the viscoplastic deformation in high-temperature forging of Ti-5.5Al-4.0Sn-4.0Zr-0.3Mo-1.0Nb-0.5Si titanium alloy, utilizing the evolution of mean grain size to characterize the resulting flow softening (Ref 3). Researchers have established many empirical and semi-empirical constitutive relationships using regression methods. However, the results have not been satisfactory because (a) the experimental data on flow stress generally contains random, unavoidable noise and (b) some unknown, nonlinear relationships may exist between flow stress, microstructure, and process parameters, which are difficult to fit into any simple pattern.

Artificial neural network theory (Ref 4) was developed on the basis of the "synapse hypothesis," i.e., the procedures of biological neural networks while information from the outside environment is learned. The artificial neural network is an information-treatment system with characteristics of adaptive learning. This method is especially suitable for treating nonlinear phenomena and complex relationships and has been applied successfully to the prediction and control of nonlinear systems and systems with unknown models (Ref 4). Li et al. applied an artificial neural network to acquire the constitutive model of flow stress in high-temperature deformation of the Ti-5Al-2Sn-2Zr-4Mo-4Cr alloy (Ref 5).

In this paper, a fuzzy set and an artificial neural network have been applied to acquire the constitutive model in the high-temperature deformation of titanium alloys. An adaptive flow stress model of Ti-6.29Al-2.71Mo-1.42Cr alloy has been established using the data from the teaching sample obtained from isothermal compression of the Ti-6.29Al-2.71Mo-1.42Cr alloy. By comparison of the calculated flow stress with the experimental data of the Ti-6.29Al-2.71Mo-1.42Cr alloy, it has been verified that the present model has good learning precision and good generalization. Therefore, it can be used to predict accurately the flow stress of the Ti-6.29Al-2.71Mo-1.42Cr alloy.

## 2. Adaptive Constitutive Model for High-Temperature Deformation

The back-propagation network (BP network) in artificial neural networks is especially suitable for treating nonlinear systems (Ref 4), and the fuzzy set can be used to represent the fuzzy characteristics in plastic deformation (Ref 6).

An adaptive constitutive model structure of the flow stress in the high-temperature deformation of titanium alloys is shown in Fig. 1, in terms of the fuzzy set and artificial neural network. In this model structure in Fig. 1, three inputs are for the deformation temperature ($T$, K), the strain rate ($\dot{\varepsilon}$, $s^{-1}$), and the strain ($\varepsilon$), one output is for the flow stress in plastic deformation, and $n$ (>3) neurons were used in the hidden layer.

The activation function in the output layer of the model obeys a linear function. The activation function in the hidden layer was selected to be a sigmoid function:

$$\mu_{A_j^i} = \exp[-(x_j - a_j^i)^2 / b_j^i] \quad \text{(Eq 1)}$$

**M.Q. Li, Aiming Xiong,** and **Xiaoli Li,** School of Materials Science and Engineering, Northwestern Polytechnical University, Xi'an, 710072, P.R. China. Contact e-mail: honeymli@nwpu.edu.cn.

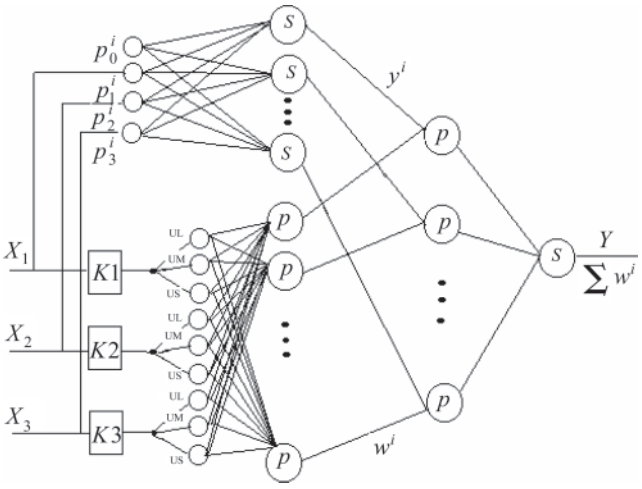


**Fig. 1** Model structure of the flow stress in high-temperature deformation

For the total output of the model structure:

$$\sigma_c\ (\text{MPa}) = \frac{\sum_{i=1}^{m} [\mu_{A_1^i}(T)\mu_{A_2^i}(\dot{\varepsilon})\mu_{A_3^i}(\varepsilon)(p_0^i + p_1^i T + p_2^i \dot{\varepsilon} + p_3^i \varepsilon)]}{\sum_{i=1}^{m} [\mu_{A_1^i}(T)\mu_{A_2^i}(\dot{\varepsilon})\mu_{A_3^i}(\varepsilon)]} \quad \text{(Eq 2)}$$

The neural networks need to be trained in a learning process before application, and the BP learning algorithm applied in the present work has to follow the tasks described below.

### *Task 1*

Task 1 determined the architecture of the fuzzy set and artificial neural networks (fuzzy neural networks) used to acquire the relationships between the flow stress and the process parameters in the high-temperature deformation of the Ti-6.29Al-2.71Mo-1.42Cr alloy shown in Fig. 1.

### *Task 2*

The fuzzy subset of process parameters with large {*UL*}, middle {*UM*}, and small {*US*} in the high-temperature deformation of the Ti-6.29Al-2.71Mo-1.42Cr alloy was regulated and shown in Fig. 2.

The subject functions are as follows.

For the deformation temperature:

$$UL1(x) = \begin{cases} 1 & x > 1223 \\ \exp\left[\dfrac{-(x-1223)^2}{6100}\right] & x \le 1223 \end{cases} \quad \text{(Eq 3a)}$$

$$UM1(x) = \exp\left[\frac{-(x-1180)^2}{1880}\right] \quad \text{(Eq 3b)}$$

$$US1(x) = \begin{cases} 1 & x < 1073 \\ \exp\left[\dfrac{-(x-1073)^2}{6100}\right] & x \ge 1073 \end{cases} \quad \text{(Eq 3c)}$$

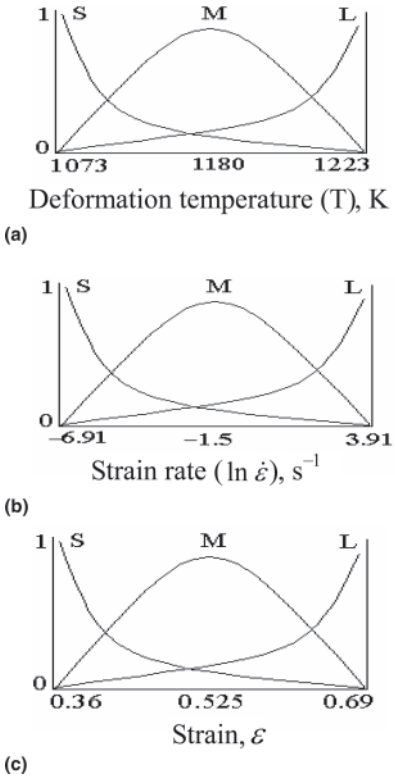


**Fig. 2** Parted sections of fuzzy set for the process parameters: (a) deformation temperature (*T*, K); (b) strain rate (ln $\dot{\varepsilon}$, $s^{-1}$); (c) strain ($\varepsilon$)

For the strain rate:

$$UL2(x) = \begin{cases} 1 & x > 3.91 \\ \exp\left[\dfrac{-(x-3.91)^2}{30}\right] & x \le 3.91 \end{cases} \quad \text{(Eq 4a)}$$

$$UM2(x) = \exp\left[\frac{-(x+1.5)^2}{10}\right] \quad \text{(Eq 4b)}$$

$$US2(x) = \begin{cases} 1 & x < -6.91 \\ \exp\left[\dfrac{-(x+6.91)^2}{30}\right] & x \ge -6.91 \end{cases} \quad \text{(Eq 4c)}$$

For the true strain:

$$UL3(x) = \begin{cases} 1 & x > 0.69 \\ \exp\left[\dfrac{-(x-0.69)^2}{0.03}\right] & x \le 0.69 \end{cases} \quad \text{(Eq 5a)}$$

$$UM3(x) = \exp\left[\frac{-(x-0.525)^2}{0.01}\right] \quad \text{(Eq 5b)}$$

$$US3(x) = \begin{cases} 1 & x < 0.36 \\ \exp\left[\dfrac{-(x-0.36)^2}{0.03}\right] & x \ge 0.36 \end{cases} \quad \text{(Eq 5c)}$$

The 27 rules obtained from the fuzzy set are described by the equations that follow.

For fuzzy rule $R^1$:

If $T$ is $UL1$, $\dot{\varepsilon}$ is $UL2$, $\varepsilon$ is $UL3$, then $\sigma_c^{F^1} = p_0^1 + p_1^1 T + p_2^1 \dot{\varepsilon} + p_3^1 \varepsilon$.

For the fuzzy rule $R^{27}$:

If $T$ is $US1$, $\dot{\varepsilon}$ is $US2$, $\varepsilon$ is $US3$, then $\sigma_c^{F^{27}} = p_0^{27} + p_1^{27} T + p_2^{27} \dot{\varepsilon} + p_3^{27} \varepsilon$.

#### Task 3

The fuzzy neural network was provided with output and input vectors.

#### Task 4

A group of variables $(x_1^0, x_2^0 \ldots, x_{n_0}^0)$ was input.

#### Task 5

The output of the network $(S_1^N, S_2^N, \ldots, S_{n_N}^N)$ was computed for a given input. All units on successive layers were updated by:

$$S_i^n = \exp[-E_i^n - a_j^i)^2 / b_j^i \quad \text{(Eq 6)}$$

$$E_i^n = \sum_{j=1}^{n_N - 1} [W_{ij} S_j^{n-1} - Q_i^n] \quad \text{(Eq 7)}$$

where $N$ is output layer with $n$ points, $Q_i^n$ is the threshold of the $i$th unit on the $n$th layer, $E_i^n$ is total of inputs of $i$th point on the $n$th layer, $j$ is a point on the hidden layer, and $W_{ij}$ are the weights between the $i$th point on the $n$th layer and the $j$th point on the $(n-1)$th layer.

#### Task 6

The average squared error between the experimental and the estimated values was computed by:

$$E = \frac{1}{2} (\sigma_e - \sigma_c)^2 \quad \text{(Eq 8)}$$

#### Task 7

Weights and thresholds were updated. This was accomplished by computing the weights and thresholds on the output layer first, and then propagating it backward through the network, layer by layer, using:

$$p_j^i(k+1) = p_j^i(k) - a(\sigma_e - \sigma_c) w^i / \sum_{i=1}^{m} w^i x_j^i \; (j = 1, 2, 3) \quad \text{(Eq 9)}$$

$$a_j^i(k+1) = a_j^i(k) - 2\beta(\sigma_e - \sigma_c) \left[ \sigma_c^i \sum_{i=1}^{m} w^i - \sum_{i=1}^{m} w^i \sigma_c^i \right] (x_j - a_j^i)^2 w^i / \left[ b_j^i \left( \sum_{i=1}^{m} w^i \right)^2 \right] \quad \text{(Eq 10)}$$

$$b_j^i(k+1) = b_j^i(k) - 2\beta(\sigma_e - \sigma_c) \left[ \sigma_c^i \sum_{i=1}^{m} w^i - \sum_{i=1}^{m} w^i \sigma_c^i \right] (x_j - b_j^i)^2 w^i / \left[ b_j^i \left( \sum_{i=1}^{m} w^i \right)^2 \right] \quad \text{(Eq 11)}$$

where $k$ is the number of weight updates and $\beta$ is a learning rate.

For the output layer

$$\delta_i^n = (S_i^* - S_i^N) P'(E_i^n) \quad \text{(Eq 12)}$$

and for the hidden layer

$$\delta_i^n = P'(E_i^n) \sum_{j=1}^{n+1} \delta_j^{n+1} W_{ij}^{n+1} \quad \text{(Eq 13)}$$

$$P'(E_i^n) = \delta_i^n (1 - \delta_i^n) \quad \text{(Eq 14)}$$

where $P'(E_i^n)$ is the first derivative of the function and $\delta_i^n$ is the error gradient of the $i$th unit on the $n$th layer.

#### Task 8

The process then returned to Task 4. After the weights and thresholds are adjusted for one set of training data, additional training sets can be used to further adjust all of the weights and thresholds.

## 3. Verification of the Constitutive Model

### 3.1 Experiments

Homogeneous compression experiments of the Ti-6.29Al-2.71Mo-1.42Cr alloy were carried out at a Thermecmastor-Z simulator for hot working with an optical dilatometer. The cylindrical specimens were 8.0 mm in diameter and 12.0 mm in height. Lubricant notches were machined on two ends. A matrix of nine different deformation temperatures and six different strain rates was constructed for the experiment. The nominal experimental deformation temperatures were ranged from 800 to 980 °C at an interval of 30 °C, and the strain rates were 0.001, 0.01, 0.1, 1.0, 10.0, and 50.0 $s^{-1}$ for each deformation temperature. Isothermal compression was performed to a 50% reduction in height (corresponding approximately to 0.7 of strain) at each combination of deformation temperatures and strain rates.

Typical flow stress curves in the $(\alpha + \beta)$ region and the $\beta$ region of the Ti-6.29Al-2.71Mo-1.42Cr alloy are illustrated in Fig. 3. In Fig. 3, it can be seen that the flow stress in the high-temperature deformation of Ti-6.29Al-2.71Mo-1.42Cr alloy is sensitive to strain rate and deformation temperature and that there is some dynamic softening.

### 3.2 Comparison of the Calculated and Experimental Data

To train the constitutive model, the experimental data at the deformation temperatures of 800, 860, 890, 950, and 980 °C were chosen as the "teaching samples." The remaining data from deformation temperatures 830 and 920 °C was used as the "testing samples." Figure 4 shows comparisons of the experimental results of the Ti-6.29Al-2.71Mo-1.42Cr alloy with the predicted results using the model described herein. The relative maximum difference of flow stress between the experimental data and the calculated results is less than 15.0% after the repetition training times of 634. The difference between predicted and

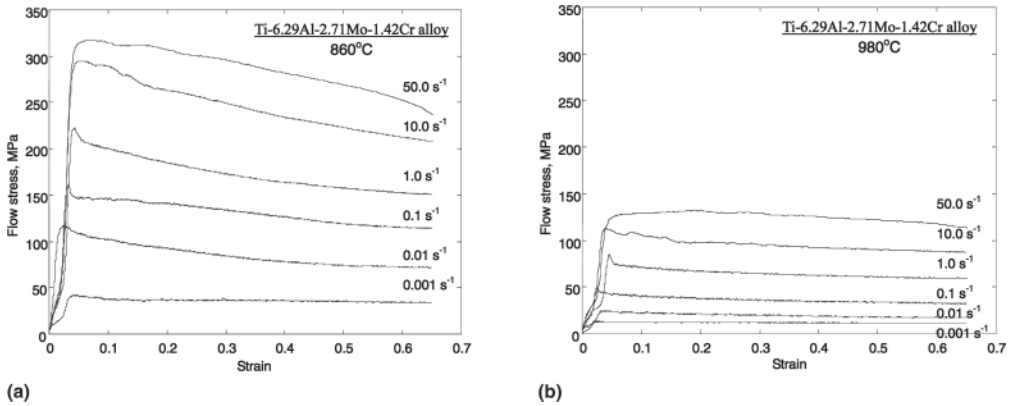


**Fig. 3** Stress-strain curves of Ti-6.29Al-2.71Mo-1.42Cr alloy during isothermal compression

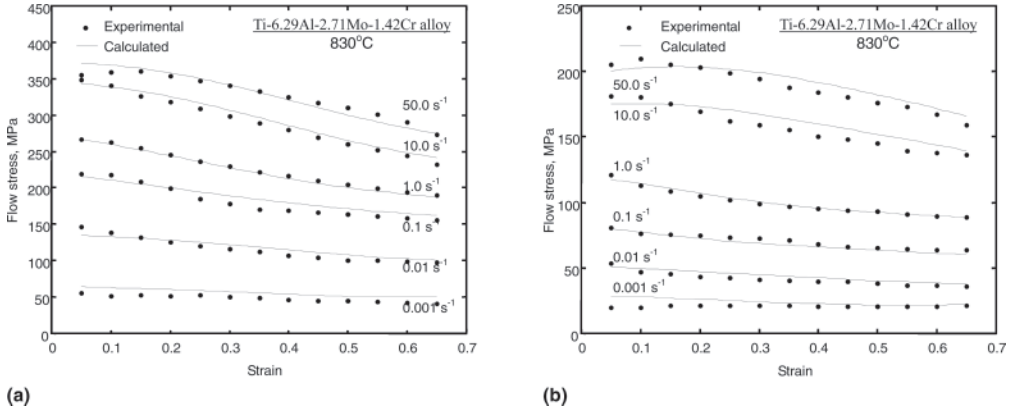


**Fig. 4** Comparison of the calculated flow stress with experimental results

experimental results gives evidence of good generalization of the present constitutive model.

## 4. Conclusions

An adaptive constitutive model for the flow stress of the Ti-6.29Al-2.71Mo-1.42Cr alloy has been established in terms of a fuzzy set and an artificial neural network. The model structure to train the fuzzy neural network feature from experimental results makes this procedure adaptive. This model was also applied to predict the flow stress of the Ti-6.29Al-2.71Mo-1.42Cr alloy in high-temperature deformation and exhibited good agreement with the experimental results.

### Acknowledgments

The authors appreciate the financial support received from the State Key Foundational Research Plan (Grant No. G2000067206) and the Teaching and Research Award Fund for Outstanding Young Teachers in Higher Education Institutions of MOE, P.R. China.

### References

1. R.C. Picu and A. Majorell, Mechanical Behavior of Ti-6Al-4V at High and Moderate Temperatures—Part II: Constitutive Modeling, *Mater. Sci. Eng. A,* 2002, 326 (2), p 306-316
2. F. Ellyin and Z. Xia, Rate-Dependent Constitutive Modelling and Micro-Mechanical Analysis of Fibre-Reinforced Metal-Matrix Composites, *J. Mech. Phys. Solids,* 2001, 49 (11), p 2543-2555
3. M. Zhou, Constitutive Modeling of the Viscoplastic Deformation in High Temperature Forging of Titanium Alloy IMI834, *Mater. Sci. Eng. A,* 1998, 245 (1), p 29-38
4. D.E. Rumelhart, G.E. Hintont, and R.J. Williams, Learning Representations by Back-Propagating Errors, *Nature,* 1986, 323, p 533-536
5. M. Li, X. Liu, S. Wu, and X. Zhang, Approach to Constitutive Relationships of a Ti-5Al-2Zr-4Cr-4Mo Alloy by Artificial Neural Networks, *Mater. Sci. Technol.,* 1998, 14 (2), p 136-138
6. M.Q. Li, A.M. Xiong, W.C. Huang, H.R. Wang, S.B. Su, and L.C. Shen, Microstructural Evolution and Modelling of the Hot Compression of a TC6 Titanium Alloy, *Mater. Charact.,* 2002, 49 (2), p 203-209